



Effect of CoFe_2O_4 weight fraction on multiferroic and magnetoelectric properties of $(1-x)\text{Ba}_{0.85}\text{Ca}_{0.15}\text{Zr}_{0.1}\text{Ti}_{0.9}\text{O}_3 - x\text{CoFe}_2\text{O}_4$ particulate composites

Ajith S. Kumar¹ · C. S. Chitra Lekha¹ · S. Vivek¹ · K. Nandakumar² · M. R. Anantharaman³ · Swapna S. Nair¹ 

Received: 9 November 2018 / Accepted: 13 March 2019 / Published online: 20 March 2019
© Springer Science+Business Media, LLC, part of Springer Nature 2019

Abstract

Different compositions of the composite lead-free multiferroic magnetoelectric systems are fabricated by employing piezoelectric $\text{Ba}_{0.85}\text{Ca}_{0.15}\text{Zr}_{0.1}\text{Ti}_{0.9}\text{O}_3$ (BCZT) and magnetostrictive CoFe_2O_4 (CFO) by varying the CFO weight fraction. The magnetic, dielectric, ferroelectric and magnetoelectric (ME) properties of the system are analyzed and found to be varying with the ferrite concentration. Even though the composite systems exhibit high magnetocapacitance (MC) properties (~35%), the possible stray contributions from magnetoresistance and magnetostriction make it unreliable for the quantitative determination of ME coupling coefficient (MECC). Therefore, a dynamic method is chosen for the measurement of magnetoelectric coupling. All the compositions have shown fairly good ME coupling. It is found that the ME coupling increases with ferrite fraction and the highest ME coupling of 14.8 mV/(cm Oe) is observed for 0.6BCZT–0.4CFO composite. It is also observed that the ME voltage increases linearly with the ac modulating field with a voltage generation of 1.25 V/cm (for $x=0.4$) for a small ac modulating field of 100 Oe. This high sensitivity and linear response of ME coupling to the ac magnetic fields offer the possibility of employing these particulate composites for a wide range of applications from magnetic field sensors to energy harvesters.

1 Introduction

Research on novel functional materials like magnetoelectric multiferroics attracts significant interest, due to its profound physics behind them as well as the large application potentials specifically in the field of energy harvesters [1–3], magnetoelectric sensors [4, 5] and storage devices [6, 7]. This special class of material exhibits both ferroelectric and magnetic properties in a single material or in an artificially engineered composite [8]. Beyond the concurrent existence

of several order parameters in a single component, the switching of magnetic or electric polarization by the other's conjugate field can involve in the development of low-power consuming multifunctional memory devices, which can have the best properties of FeRAMs and MRAMs [9]. In single phase multiferroics, such as bismuth ferrite (BFO) [10, 11], the ME coupling is often due to the local interaction between the ordered ferroelectric and magnetic sublattices. They, however, exhibit weak coupling properties at room temperature [12], making them unusable for any practical applications. To obtain better ME coupling, an alternative strategy is to fabricate artificial heterostructures consisting of ferroelectric and magnetic phases [8, 13, 14]. In this kind of heterostructures, individual phases can be separately optimized for achieving high ME coupling at room temperature.

Magnetoelectric particulate composites belong to the class of engineered artificial systems, where the coupling is achieved via strain-mediated mechanical interaction at the piezoelectric/magnetostrictive interfaces. Since ME coupling is a product property, the piezoelectric constant and magnetostrictive properties of the individual ferroelectric and magnetic phases should be very high in order to obtain high coupling. Along with the high ferroic properties, the

Electronic supplementary material The online version of this article (<https://doi.org/10.1007/s10854-019-01140-3>) contains supplementary material, which is available to authorized users.

✉ Swapna S. Nair
swapna.s.nair@gmail.com

¹ Dept. of Physics, Central University of Kerala, Kasaragod 671316, India

² Dept. of Physics, Mahatma Gandhi University, Kottayam 686560, India

³ Dept. of Physics, Cochin University of Science and Technology, Kochi 682022, India

connectivity schemes and weight ratios also play crucial roles in determining the strength of coupling between the two phases. High ME coupling values have been reported for the composites comprising of most promising piezoelectric candidates such as PZT, PMN-PT, and ferrites such as NiFe_2O_4 (NFO) and CoFe_2O_4 (CFO) [15–17]. These systems, however, contain lead, which is known for its highly poisonous nature. Hence the development of lead-free electronics is become the need of the hour. As a lead-free perovskite, BaTiO_3 (BTO) is actively involved in many ME systems and is found to have very high coupling coefficient as high as 140 mV/(cm Oe) for the bulk particulate composites [18–20].

Recently, a new derivative of BTO called BCZT ($\text{Ba}_{0.85}\text{Ca}_{0.15}\text{Zr}_{0.1}\text{Ti}_{0.9}\text{O}_3$) is recognized to have high piezoelectric constant ($d_{33} \sim 600$ pC/N) at room temperature [21]. The superior piezoelectric property of BCZT is due to the low crystalline anisotropy and high elastic compliances in the rhombohedral–tetragonal (R–T) phase transition region. Also, this particular composition of BCZT offers an excellent electromechanical coupling property which is desirable to act as an active component in multiferroic magnetoelectric composites.

Hence, a multiferroic composite employing BCZT as the piezoelectric phase is expected to have better ME coupling properties. However, there are not many ME systems were reported with BCZT as the piezoelectric component. Therefore, it is essential to explore the potential of BCZT in providing adequate ME coupling in composite multiferroic systems.

CFO is a highly magnetostrictive material along with high piezomagnetic and coupling coefficient [22]. These properties are desirable for obtaining high ME coupling. Therefore, CFO is a widely used magnetostrictive candidate for heterostructured ME composites [17, 23, 24]. Here, authors fabricated magnetoelectric particulate composites of lead-free piezoelectric, $\text{Ba}_{0.85}\text{Ca}_{0.15}\text{Zr}_{0.1}\text{Ti}_{0.9}\text{O}_3$ and magnetostrictive ferrite, CoFe_2O_4 . The composite systems have the general formula, $(1-x)\text{BCZT} - x\text{CFO}$. The weight fraction of CFO is varied from $x=0.1$ to 0.5 so that the ME coupling properties can be tailored by varying the composition. In addition to the magnetoelectric coupling properties, the magnetic properties, ferroelectric properties, dielectric properties as well as the magneto-dielectric properties are also systematically studied.

2 Experimental

Stoichiometric amounts of Barium carbonate, Calcium carbonate, Zirconium oxide, and Titanium dioxide were added in a tungsten carbide vial and ball milled for 30 min using tungsten carbide balls in acetone medium. The obtained slurry was heated in an oven at 70 °C and grounded well

using an agate mortar and pestle. The as-prepared powder was sintered at 1200 °C to get BCZT powders. Nitrate based sol–gel method was selected for the synthesis of CFO. A stoichiometric amount of Cobalt nitrate and Ferric nitrate were dissolved in Ethylene glycol. The sol was heated at 60 °C using a hot plate to get a gel, followed by firing at 200 °C. Black powder was obtained as a result of this self-combustion process. The as-synthesized powder was ground well and annealed at 900 °C. For the fabrication of the composite systems, the annealed powders of BCZT and CFO were taken in different weight proportions and ball milled for 30 min in acetone medium. The obtained particulate composites were made into a pellet using a uniaxial pellet press and sintered at 1200 °C for densification. For electrical measurements, the silver paste was applied on both sides of pellets for making good electrical contacts.

The X-Ray diffractograms of samples were recorded using Rigaku Miniflex 600, with Cu-K α radiation ($\lambda = 1.5406$ Å) in theta-2theta mode. The Scanning Electron Micrographs were obtained by employing field emission scanning electron microscopy (FESEM, Zeiss Sigma). The magnetization studies were carried out using the VSM module of PPMS (VersaLab, Quantum Design). The ferroelectric polarization of the samples was measured using a PE loop tracer (Precision LC, Radiant). The magnetocapacitance properties were analyzed using an Impedance analyzer (Wayne-Kerr 6500B) together with an electromagnet. The dynamic magnetoelectric effect was studied in an ME coupling measurement setup (Marine India) consisting of Helmholtz coil, signal generator, and a DC electromagnet.

3 Results and discussion

3.1 Structural properties

Figure 1a shows the X-Ray diffraction (XRD) patterns of composite powders. The XRD patterns confirm the coexistence of both inverse spinel CFO and perovskite BCZT. No visible impurity peaks were observed in XRD, which hints towards the mutual insolubility between the two phases in the composites even after the intermixing and the sintering process. However, in addition to the most intense peak at 31.5° (cubic 110), we have observed the emergence of another peak, which can be identified as the tetragonal (101) peak of the BCZT (Fig. 1b). The splitting is found to be increased with the increase in the CFO weight fraction. This induced tetragonality can be attributed to the formation of strain due to the intermixing of different phases.

The SEM images of the $(1-x)\text{BCZT} - x\text{CFO}$ composite systems are shown in Fig. 2a–e. Almost all the samples show a uniform distribution of constituent grains. It is also clear that the samples are not so dense, as some pores/

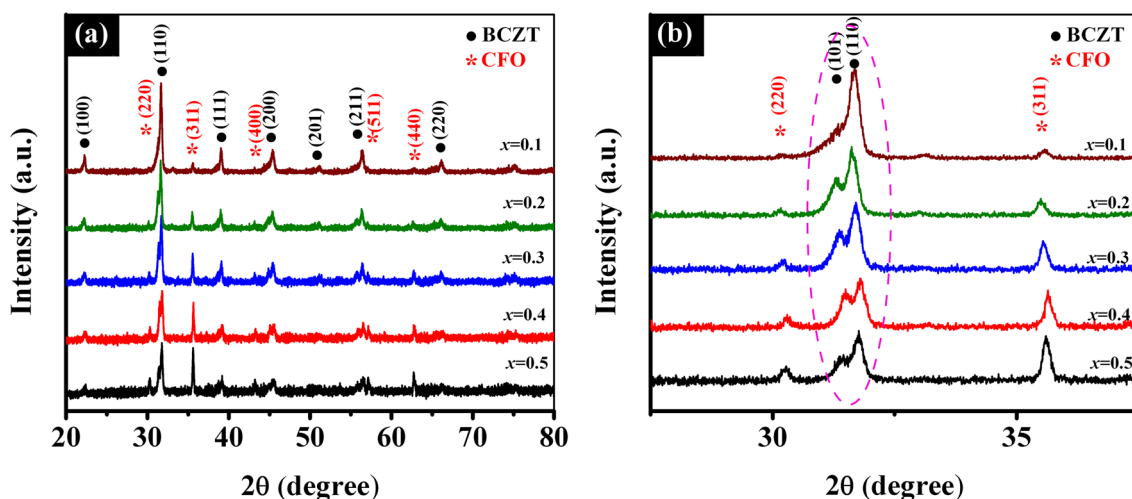


Fig. 1 **a** X-ray diffraction patterns of $(1 - x)$ BCZT – x CFO composite powders. **b** Zoomed version of XRD showing the splitting of cubic phase to tetragonal phase

voids are visible in the SEM images. In order to verify the compositional consistency; we have performed the EDX (Energy dispersive X-ray spectroscopy) analysis (Fig. 2f) of the samples and compared with the theoretical values. The theoretical atomic percentage was calculated using the compositional formula $(1 - x)$ BCZT – x CFO and the results are given in Table 1.

3.2 Multiferroic properties

Figure 3a, b shows the M-H hysteresis loop of $(1 - x)$ BCZT – x CFO composites at room temperature (300 K) and at low temperature (60 K). All the samples showed well-defined hysteresis loops, confirming the ferromagnetic behavior of the composites. The variation of the magnetization with the weight fraction of CFO is given in the inset of Fig. 3a. It can be easily observed that the saturation magnetization increases with the increasing ferrite concentration which is assigned to the low concentration effect of the nonmagnetic contributor. All compositions have obeyed the rule of mixtures. However, the saturation magnetization of pure CFO predicted by the rule of mixtures is ≈ 72.7 emu/g, which is greater than the obtained value of 67.3 emu/g. The coercivity also decreases with ferrite concentration. This variation from the rule of mixtures and the reduction in coercivity may be due to either (i) the mechanical coupling between the piezoelectric and the magnetic phases or (ii) the strain introduced to the system during the milling and sintering processes or both.

At low temperatures, the saturation magnetization and coercivity for all the samples are found to be increased compared to their room temperature values. This is due to the reduced thermal fluctuations with the reduction in thermal

energy as expected. The reduction in thermal energy causes the magnetic domains to reorient along the applied field. Thus, the low temperature characterization plays an essential role to understand the underlying magnetic phenomena of the composites in detail.

The ferroelectric hysteresis behavior of the composites for different ferrite weight fractions is shown in Fig. 3c. It is observed that the polarization values decrease with the increase in ferrite weight fraction. A plot of remnant polarization as a function of ferrite concentration is shown in Fig. 3d. The remanence slightly changes as we go from $x=0.1$ to $x=0.2$ followed by a large drop at $x=0.3$. This can be explained in view of the lossy nature of the composites which increases with the incorporation of more conducting ferrite particles. Ferroelectric behavior is characterized by the ordered arrangement of electric dipoles in the system. The presence of ferrites, however, disrupts the long range ordering of electric dipoles and thus can reduce the electric polarization. When a ferroelectric matrix is embedded with more and more ferrite particles, the ferroelectric polarization decreases [17].

3.3 Dielectric and magnetocapacitance properties

The dielectric response (Fig. 4a) of all the compositions with respect to frequency shows a rapid decrease in the dielectric constant (ϵ_r) in the low-frequency region and exhibits almost independent behavior at higher frequencies. This behavior can be explained with the help of the Maxwell–Wagner model for dielectrics [25]. This model demonstrates the dielectric material as an assembly of well-conducting grains in a matrix of non-conducting grain boundaries. On the application of an electric field,

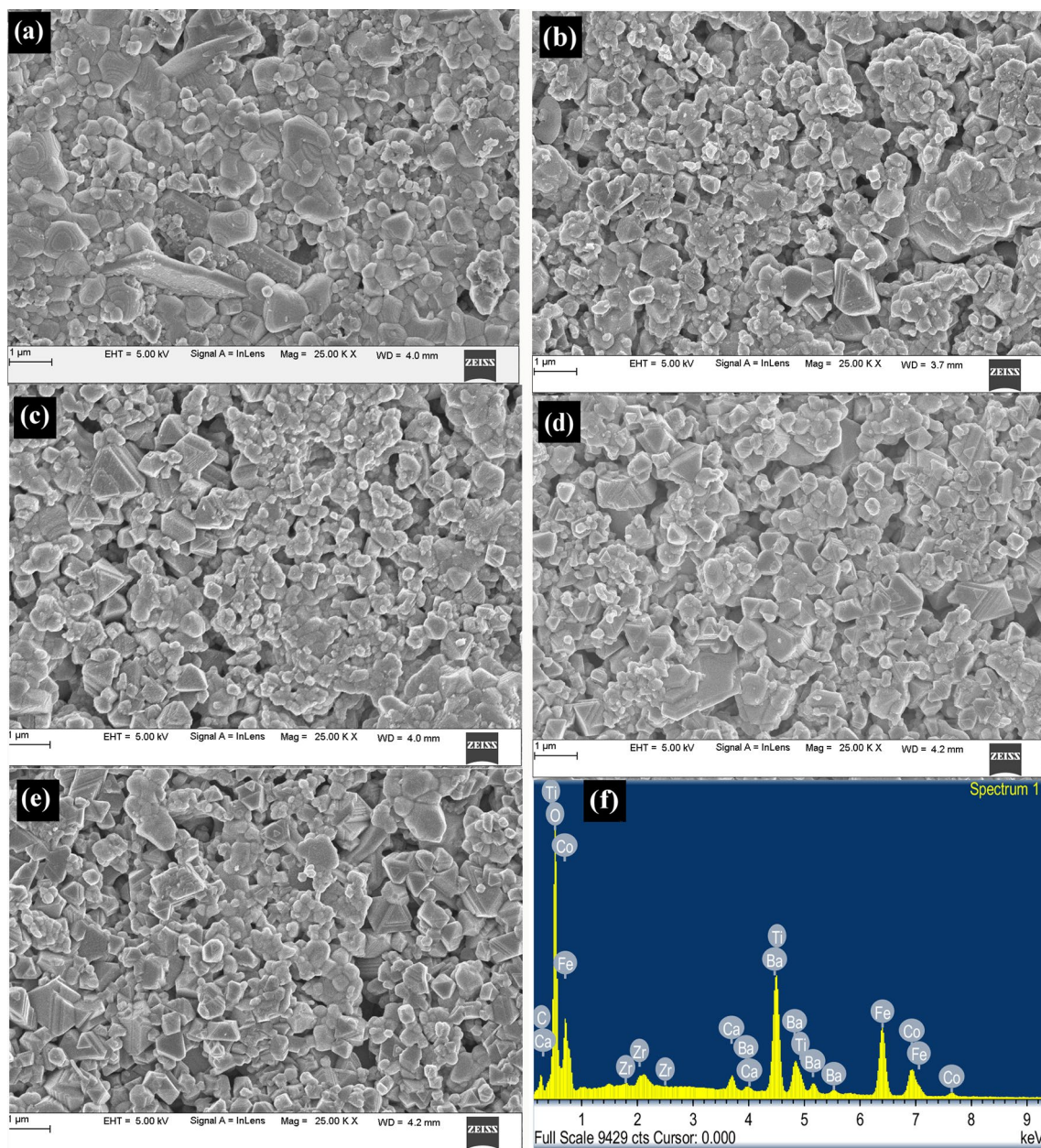


Fig. 2 a–e SEM images of the composites for $x=0.1$ to $x=0.5$. f EDX spectrum of 0.5 BCZT – 0.5 CFO composite

the charges will be accumulated in the grain–grain boundary interfaces due to the poor conductivity of grain boundaries, resulting in an interfacial polarization. The accumulated charges can easily follow the electric field with low frequencies. As the frequency increases, charges are unable to follow the fast switching of the electric field, resulting in a reduced dielectric constant. Thus, at higher frequencies, interfacial polarization cannot contribute to the dielectric properties and the entire contribution is from the intrinsic electronic polarizability of the material.

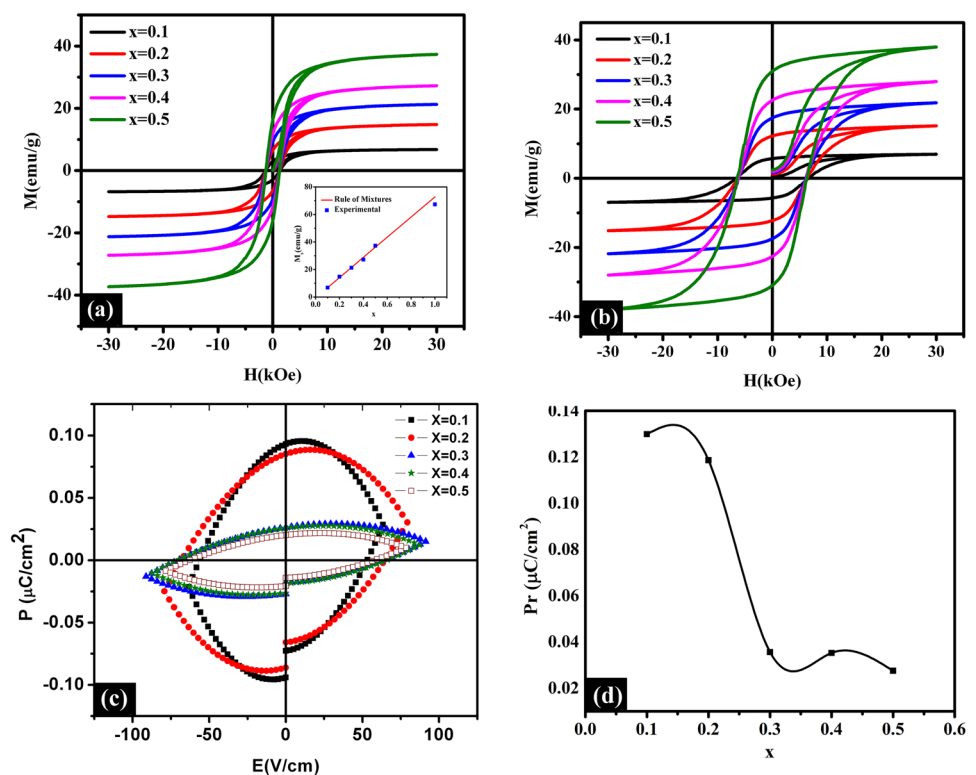
It is also evident from the figure that the ϵ_r monotonically decreases with ferrite concentration. One might expect an increase in the dielectric permittivity with CFO concentration, due to an enhanced Maxwell–Wagner type interfacial polarization as the number of interfaces increases with the incorporation of comparatively smaller particle size of CFO. However, in the current investigation, the porosity of the composites (which is evident from the SEM images) and the relatively higher conductivity of ferrite phase cause a decrease in dielectric constant (ϵ_r) as observed. The reduction in ϵ_r is more

Table 1 The composition of the $(1-x)\text{BCZT} - x\text{CFO}$ composite systems: showing the comparison between the theoretical and experimental atomic percentage. It can be observed that within the limit of

experimental error, the atomic percentage, which was used during the synthesis, is in good agreement with the experimental results

Element	$x=0.1$		$x=0.2$		$x=0.3$		$x=0.4$		$x=0.5$	
	Experiment	Theory	Experiment	Theory	Experiment	Theory	Experiment	Theory	Experiment	Theory
O	65.40	59.71	64.57	59.43	65.52	59.14	66.80	58.86	66.04	58.57
Ca	2.31	2.70	1.92	2.40	1.63	2.10	1.29	1.80	1.02	1.50
Ti	12.82	16.20	11.01	14.40	8.87	12.60	7.54	10.80	6.15	9.00
Fe	3.16	2.86	6.42	5.71	8.87	8.57	10.99	11.43	13.54	14.29
Co	1.84	1.43	3.31	2.86	4.47	4.29	5.43	5.71	6.53	7.14
Zr	1.09	1.80	0.85	1.60	0.76	1.4	0.51	1.2	0.39	1
Ba	13.38	15.30	11.93	13.60	9.88	11.9	7.44	10.2	6.33	8.5
Total	100	100	100	100	100	100	100	100	100	100

Fig. 3 M–H hysteresis loops of $(1-x)\text{BCZT} - x\text{CFO}$ particulate composites **a** at 300 K and **b** at 60 K. Inset of **a** shows the variation of saturation magnetization with the CFO weight fraction. **c** Polarization versus Electric field hysteresis loops of composites with different ferrite concentrations. **d** Variation of remnant polarization as a function of CFO weight fraction



evident at low frequencies, while at higher frequencies the ϵ_r shows only a slight decrease due to the reduced contribution of interfacial polarization. Dipolar and interfacial polarization lag behind the applied frequencies above 100 kHz ~ 1 MHz range. At this higher frequency range, the electronic polarization dominates, which is almost independent of the variation in ferrite weight fraction. This is also evident from the frequency response of the loss-tangent for various ferrite concentrations (Fig. 4b). As the ferrite concentration increases, the peak of dielectric loss is shifted towards the low-frequency region. This again confirms that the low-frequency dielectric response is mostly influenced by the ferrite weight percentage than the

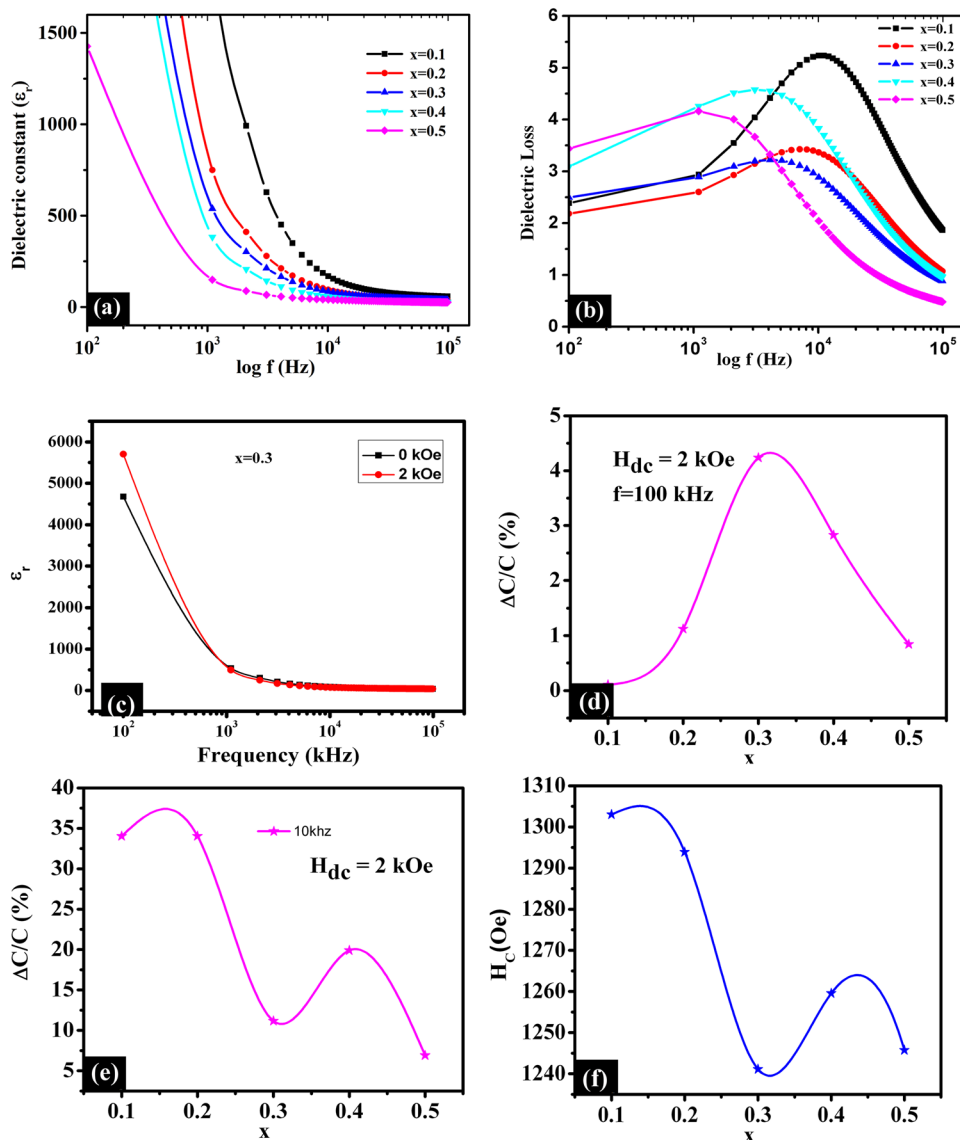
number of interfaces due to the difference in conductivity of the constituent phases.

Figure 4c shows the magnetocapacitance (MC) properties of the 0.7 BCZT–0.3CFO composite. The magnetocapacitance effect is defined as,

$$MC(\%) = \frac{C(H) - C(H = 0)}{C(H = 0)} \times 100 \quad (1)$$

where, $C(H)$ is the capacitance at an applied magnetic field H and $C(H = 0)$ is the dielectric permittivity at zero magnetic fields.

Fig. 4 **a** Variation dielectric constant as a function of frequency. **b** Dielectric loss as a function of frequency, **c** Magnetocapacitance for $x=0.3$, **d** Magnetocapacitance as a function of ferrite concentration at 100 kHz, **e** Magnetocapacitance at 10 kHz, **f** Variation of coercivity as a function of ferrite concentration



At a low frequency of 10 kHz, the magnetocapacitance reaches as high as $\sim 35\%$ for $x = 0.1$ and $x = 0.2$ (Fig. 4e). However, the magnetocapacitance varies non-monotonically with ferrite concentration. This is interesting, as the variation of MC with ferrite concentration actually keeps a one to one correspondence with the magnetic coercivity vs. ferrite concentration (Fig. 4f). Since CFO is an intrinsically magnetostrictive material; it can induce dimensional changes to the samples in the presence of an applied magnetic field and can result in a pseudo-magnetocapacitance effect [26]. Thus, we can assume that the observed low-frequency MC response is mostly due to the presence of the ferrite phase, which has nothing to do with magnetoelectric (ME) coupling. The MC at a higher frequency of 100 kHz (Fig. 4d), gives an appreciable response of $\approx 4.5\%$ for $x = 0.3$. The high frequency MC response initially increases with ferrite concentration and then decreases. This behavior is analogous to the ME

coupling behavior of the composites, which will be discussed following section. Even though the MC effect can be due to ME coupling, it can also be due to magnetoresistance as well as the dimensional changes in the samples. Thus, one can use MC studies only as a probe to qualitatively identify the magnetoelectric properties in multiferroic ME systems, as the method is not false-proof.

3.4 Magnetoelectric coupling properties

Static methods like magnetocapacitance measurements are not free from errors because of the overlap of the Hall signals, magnetoresistance, and stray dc signals and hence cannot be used for exclusive quantification of magnetoelectric effect [8], as we have already seen in the previous discussion (Sect. 3.3). In order to avoid the contributions from these erroneous sources, we have adopted

a dynamic measurement, where an alternating magnetic field is employed for modulating the magnetic phase during the measurement. The voltage developed in the sample here is measured by a lock-in amplifier, whose frequency is locked to the ac modulating frequency of the Helmholtz coil. Hence, all other contributions to the voltage will be discarded and the measured signal will be consisting only of an alternating voltage, purely due to the magnetoelectric effect.

The magnetoelectric coupling coefficient (MECC) is defined as the ratio of ME voltage (dV) to the product of the thickness (t) and the modulating ac magnetic field (H_{ac}). It is given by,

$$MECC = \frac{dV}{t.H_{ac}} \quad (2)$$

The ME coupling in magnetostrictive-piezoelectric composites can be explained on the basis of interfacial mechanical coupling between the constituent phases in the system. The strain induced in the magnetostrictive phase, by an applied magnetic field, will be transferred to the piezoelectric phase via mechanical coupling between them. This strain will generate a voltage in the piezoelectric phase due to the piezoelectric effect (Eq. (3)) [8]. In effect, the applied magnetic field has generated a voltage in the composite system via magnetoelectric effect. Thus, the area of contact between the phases plays an important role in this kind of strain mediated ME coupling. In particulate composites, like the present system, we would not expect a very high ME coupling due to the small area of contact, arising from the shape of the constituent phases, the random orientation of phases and due to the porosity of the composite pellets.

$$MECC = \frac{\text{Magnetic field}}{\text{Strain}} \times \frac{\text{Strain}}{\text{Piezoelectric Voltage}} \quad (3)$$

Since the ME coupling is strain mediated, the nature of the change in the magnetostriction of the ferrite phase will be directly reflected in it. The change in magnetostriction with the applied magnetic field can be deduced from the virgin curve of the M-H plot as given by the Eq. (4) [27, 28]. The M^2 and dM^2/dH as a function of the magnetic field are shown in Fig. 5. It is evident from the figures (Figs. 5, 6) that the ME coupling maintains a one to one correspondence with magnetostriction behavior.

$$\frac{d\lambda}{dH} \propto \frac{dM^2}{dH} \quad (4)$$

where λ is the magnetostriction, M is the magnetization and H is the applied magnetic field.

The dc bias field dependence of the MECC for all compositions is shown in Fig. 6a–e. The MECC initially increases with the bias field and then decreases after passing through a maximum. As we apply the dc magnetic field, the magnetic

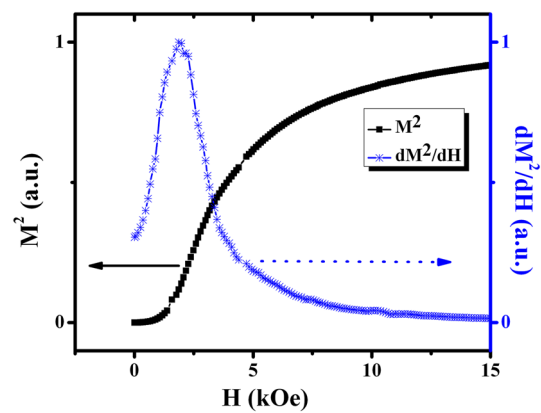
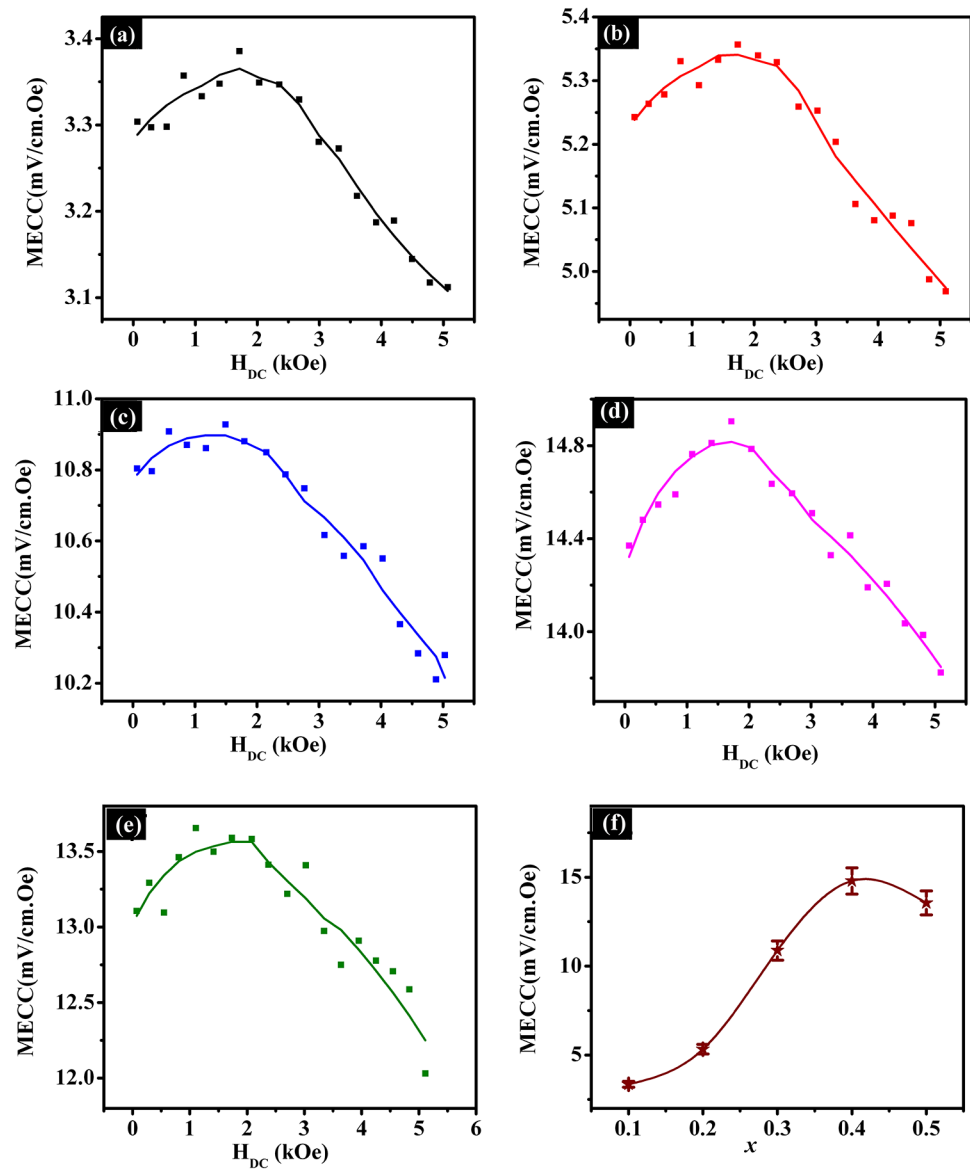


Fig. 5 Plot of M^2 vs. H and dM^2/dH vs. H . The magnetostriction (λ) is proportional to the square of the magnetization, M^2 as given in Eq. (2)

moments start to align along the bias field, resulting in a dimensional change (magnetostriction) in the magnetic phase due to the spin–orbit coupling. Due to magnetocrystalline anisotropy, the magnetostriction has different magnitudes and has opposite directions along easy and hard axes. The total magnetostriction is the sum of the easy axis and hard axis magnetostriction [29, 30]. As a result, the easy axis magnetostriction, which dominates in the low field region, causes an increase in MECC. As the field increases, the influence of hard axis magnetostriction increase, which causes a decrease in MECC. Beyond the saturation, the change in magnetically induced polarization is negligible while the applied field is changing rapidly. This results in a reduced MECC at higher magnetic fields.

Figure 6f shows the variation of MECC with respect to the weight fraction of CFO. MECC increases initially with x , reaches a maximum (≈ 14.8 mV/(cm Oe)) for $x=0.4$ and then decreases. This is anticipated, as the area of contact between magnetostrictive and piezoelectric phases increases with ferrite weight fraction resulting in better strain-mediated ME coupling. The maximum coupling should correspond to the maximum area of contact between the phases which was expected for $x=0.5$ as the constituents have comparable densities. However, slight variation can happen, since the particles of the ferrite and piezoelectric phases differ in size. Lekha et al. reported a similar trend in the variation of MECC with respect to the ferrite fraction [31]. The obtained MECC has an adequate value and comparable to other particulate composite systems such as a laminated structure reported by Praveen et al. (16 mV/cm Oe at 1 kHz) and a core–shell system by our own group (12 mV/cm Oe at 50 Hz) with the same piezoelectric and ferrite materials as the constituent phases [32, 33]. However, it is less than the value reported by Wang *et al.* (159 mV/cm Oe at 1 kHz) for a trilayer laminated structure of BCZT-CFO-BCZT [34]. This is due

Fig. 6 dc bias field dependence of magnetolectric coupling coefficient (MECC) for various CFO weight fraction **a** $x=0.1$, **b** $x=0.2$, **c** $x=0.3$, **d** $x=0.4$, **e** $x=0.5$. **f** Variation of maximum MECC values with CFO weight fraction



to the better connectivity in laminated structures than in particulate composites. These systems can perform even better if operated at resonance frequencies.

The ME voltage has shown a linear dependence on the ac magnetic field, which is shown in Fig. 7. The slope of the straight line gives the ME coupling coefficient. This behavior can be predicted from the Eq. (2). These systems have developed an adequate voltage of ~ 59 mV/cm (for $x=0.4$) even at a feeble ac modulating field of 5 Oe. The voltage generation reaches as high as ~ 1.25 V/cm for 100 Oe. This high voltage generation along with the linear nature of ac field dependence of ME coupling offers a wide range of application potential for these systems ranging from magnetic field sensors to energy harvesters in MEMS and NEMS devices.

4 Conclusion

The lead-free magnetolectric particulate composites of piezoelectric BCZT and magnetostrictive CFO were fabricated and analyzed for their room temperature multiferroic and magnetolectric properties. The systems were multiferroic at room temperature. The 0.6BCZT–0.4CFO system showed the highest ME coupling with a coupling coefficient of 14.8 mV/(cm Oe) and could generate upto 1.25 V/cm for a magnetic field of 100 Oe. It was observed that the ME voltage varies linearly with the ac modulating field. The systems were sensitive to even very feeble magnetic fields as low as 5 Oe, with a voltage generation of 59 mV/cm which point towards its direct application

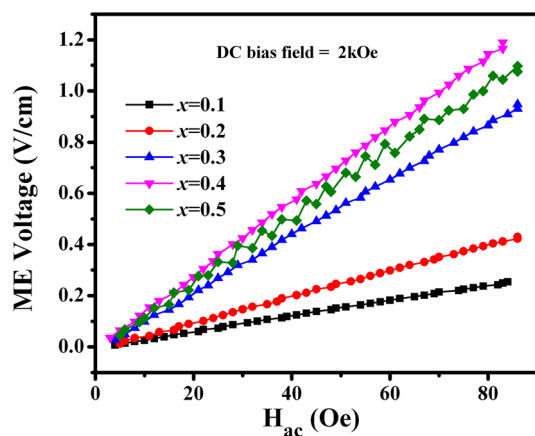


Fig. 7 ME voltage generation as a function of ac modulating field. The composite systems are sensitive to feeble magnetic fields as low as 5 Oe

in passive magnetic field and current sensing because of the linear response of the generated voltage against the ac modulating field. The investigation can also open up the possibility of developing devices based on the converse ME effects, such as magnetically and electrically tunable microwave devices and miniature antennas. By tailoring material parameters and connectivity schemes of such composite thick/thin films, further enhancement of ME coupling is expected which can enhance their application potential in different fields ranging from spintronics to medical devices.

Acknowledgements ASK, CSC, VS, and SSN acknowledge Central University of Kerala for financial support. ASK wish to acknowledge University Grants Commission, India for the Junior and Senior Research Fellowship (F.17–131/2012(SA-1) and CSC and SSN wish to acknowledge DST, India for the financial support in WOS-A (SR/WOS-A/PS-14/2014) and YSS/2014/000431. SSN acknowledge DBT, India for the financial support through the project 6292P52/RGCB/PMD/DBT/RPKT/2015.

Compliance with ethical standards

Conflict of interest Authors certify that there is no actual or potential conflict of interest in relation to this article.

References

- P. Taylor, Y. Li, X. Yang et al., One-dimensional metal oxide nanotubes, nanowires, nanoribbons, and nanorods: synthesis, characterizations, properties and applications. *Crit. Rev. Solid State Mater. Sci.* (2012). <https://doi.org/10.1080/10408436.2011.606512>
- Y. Zhu, J.W. Zu, A magnetoelectric generator for energy harvesting from the vibration of magnetic levitation. *IEEE Trans. Magn.* **48**, 3344–3347 (2012). <https://doi.org/10.1109/TMAG.2012.2199289>
- C.S.C. Lekha, A.S. Kumar, S. Vivek et al., High voltage generation from lead-free magnetoelectric coaxial nanotube arrays and their applications in nano energy harvesters. *Nanotechnology* **28**, 055402 (2017). <https://doi.org/10.1088/1361-6528/28/5/055402>
- J. Reermann, P. Durdaud, S. Salzer et al., Evaluation of magnetoelectric sensor systems for cardiological applications. *Measurement* **116**, 230–238 (2018). <https://doi.org/10.1016/j.measurement.2017.09.047>
- R. Jahns, H. Greve, E. Woltermann et al., Sensitivity enhancement of magnetoelectric sensors through frequency-conversion. *Sens. Actuators A* **183**, 16–21 (2012). <https://doi.org/10.1016/J.SNA.2012.05.049>
- W. Saenrang, B.A. Davidson, F. Maccherozzi et al., Deterministic and robust room-temperature exchange coupling in monodomain multiferroic BiFeO₃ heterostructures. *Nat. Commun.* **8**, 1583 (2017). <https://doi.org/10.1038/s41467-017-01581-6>
- M. Bibes, A. Barthélémy, Towards a magnetoelectric memory. *Nat. Mater.* **7**, 425–426 (2008). <https://doi.org/10.1038/nmat2189>
- Y. Wang, J. Hu, Y. Lin, C.-W. Nan, Multiferroic magnetoelectric composite nanostructures. *NPG Asia Mater* **2**, 61–68 (2010). <https://doi.org/10.1038/asiamat.2010.32>
- Y. Zhang, Z. Li, C. Deng et al., Demonstration of magnetoelectric read head of multiferroic heterostructures. *Appl. Phys. Lett.* **92**, 125210 (2008). <https://doi.org/10.1063/1.2912032>
- N. Kumar, A. Shukla, R.N.P. Choudhary, Structural, electrical and magnetic characteristics of Ni/Ti modified BiFeO₃ lead free multiferroic material. *J Mater Sci Mater Electron* **28**, 6673–6684 (2017). <https://doi.org/10.1007/s10854-017-6359-y>
- N. Kumar, A. Shukla, N. Kumar, R.N.P. Choudhary, Structural, electrical and magnetic properties of eco-friendly complex multiferroic material: Bi(Co_{0.35}Ti_{0.35}Fe_{0.30})O₃. *Ceram. Int.* **45**, 822–831 (2019). <https://doi.org/10.1016/J.CERAMINT.2018.09.249>
- D. Khomskii, Trend: classifying multiferroics: Mechanisms and effects. *Physics (College Park Md)* **2**, 20 (2009)
- W. Eerenstein, N.D. Mathur, J.F. Scott, Multiferroic and magnetoelectric materials. *Nature* **442**, 759–765 (2006). <https://doi.org/10.1038/nature05023>
- C.-W. Nan, M.I. Bichurin, S. Dong et al., Multiferroic magnetoelectric composites: historical perspective, status, and future directions. *J. Appl. Phys.* **103**, 031101 (2008). <https://doi.org/10.1063/1.2836410>
- J.G. Wan, X.W. Wang, Y.J. Wu et al., Magnetoelectric CoFe₂O₄–Pb(Zr,Ti)O₃ composite thin films derived by a sol-gel process. *Appl. Phys. Lett.* **86**, 122501 (2005). <https://doi.org/10.1063/1.1889237>
- A.J. Gualdi, F.L. Zabotto, D. Garcia et al., Understanding the dynamic magnetization process for the magnetoelectric effect in multiferroic composites. *J. Appl. Phys.* **119**, 124110 (2016). <https://doi.org/10.1063/1.4944889>
- L.K. Pradhan, R. Pandey, R. Kumar, M. Kar, Lattice strain induced multiferroicity in PZT-CFO particulate composite. *J. Appl. Phys.* **123**, 074101 (2018). <https://doi.org/10.1063/1.5008607>
- H. Yang, G. Zhang, Y. Lin, Enhanced magnetoelectric properties of the laminated BaTiO₃/CoFe₂O₄ composites. *J. Alloys Compd.* **644**, 390–397 (2015). <https://doi.org/10.1016/J.JALLC.OM.2015.05.020>
- B. Sarkar, B. Dalal, V. Dev Ashok et al., Magnetic properties of mixed spinel BaTiO₃-NiFe₂O₄ composites. *J. Appl. Phys.* **115**, 123908 (2014). <https://doi.org/10.1063/1.4869782>
- A.S. Gaikwad, S.E. Shirsath, S.R. Wadgane et al., Magnetoelectric coupling and improved dielectric constant of BaTiO₃ and Fe-rich (Co_{0.7}Fe_{2.3}O₄) ferrite nano-composites. *J. Magn. Mater.* **465**, 508–514 (2018). <https://doi.org/10.1016/J.JMMM.2018.06.036>

21. W. Liu, X. Ren, Large piezoelectric effect in Pb-free ceramics. *Phys. Rev. Lett.* **103**, 257602 (2009). <https://doi.org/10.1103/PhysRevLett.103.257602>
22. K.K. Mohaideen, P.A. Joy (2012) High magnetostriction and coupling coefficient for sintered cobalt ferrite derived from superparamagnetic nanoparticles High magnetostriction and coupling coefficient for sintered cobalt ferrite derived from superparamagnetic nanoparticles. *Appl. Phys. Lett.* <https://doi.org/10.1063/1.4745922>
23. F. Yan, G. Chen, L. Lu et al., Local probing of magneto-electric coupling and magnetoelastic control of switching in BiFeO₃-CoFe₂O₄ thin-film nanocomposite. *Appl. Phys. Lett.* **103**, 042906 (2013). <https://doi.org/10.1063/1.4816793>
24. M.M. Selvi, P. Manimuthu, K.S. Kumar, C. Venkateswaran, Magnetodielectric properties of CoFe₂O₄-BaTiO₃ core-shell nanocomposite. *J. Magn. Magn. Mater.* **369**, 155–161 (2014). <https://doi.org/10.1016/j.jmmm.2014.06.039>
25. C.G. Koops, On the dispersion of resistivity and dielectric constant of some semiconductors at audiofrequencies. *Phys. Rev.* **83**, 121–124 (1951). <https://doi.org/10.1103/PhysRev.83.121>
26. G. Catalan, Magnetocapacitance without magnetoelectric coupling. *Appl. Phys. Lett.* **88**, 102902 (2006). <https://doi.org/10.1063/1.2177543>
27. A.J. Gualdi, F.L. Zabotto, D. Garcia, A.J.A. de Oliveira, Stress magnetization model for magnetostriction in multiferroic composite. *J. Appl. Phys.* **114**, 053913 (2013). <https://doi.org/10.1063/1.4816785>
28. S. Ito, K. Aso, Y. Makino, S. Uedaira, Magnetostriction and magnetization of iron-based amorphous alloys. *Appl. Phys. Lett.* **37**, 665–666 (1980). <https://doi.org/10.1063/1.92029>
29. A. Muhammad, R. Sato-Turtelli, M. Kriegisch et al., Large enhancement of magnetostriction due to compaction hydrostatic pressure and magnetic annealing in CoFe₂O₄. *J. Appl. Phys.* **111**, 013918 (2012). <https://doi.org/10.1063/1.3675489>
30. R.M. Bozorth, E.F. Tilden, A.J. Williams, Anisotropy and magnetostriction of some ferrites. *Phys. Rev.* **99**, 1788–1798 (1955). <https://doi.org/10.1103/PhysRev.99.1788>
31. C.S.C. Lekha, A.S. Kumar, S. Vivek et al., Room temperature magnetoelectric properties of lead-free alkaline niobate based particulate composites. *Ceram. Int.* (2019). <https://doi.org/10.1016/J.CERAMINT.2019.01.089>
32. A.S. Kumar, C.S.C. Lekha, S. Vivek et al., Multiferroic and magnetoelectric properties of Ba_{0.85}Ca_{0.15}Zr_{0.1}Ti_{0.9}O₃-CoFe₂O₄ core-shell nanocomposite. *J. Magn. Magn. Mater.* **418**, 294–299 (2016). <https://doi.org/10.1016/j.jmmm.2016.02.065>
33. J. Paul Praveen, V.R. Monaji, E. Chandrakala et al., Enhanced magnetoelectric coupling in Ti and Ce substituted lead free CFO-BCZT laminate composites. *J. Alloys Compd.* **750**, 392–400 (2018). <https://doi.org/10.1016/J.JALLCOM.2018.04.026>
34. Y. Wang, Y. Pu, Y. Shi, Y. Cui, Ferroelectric, magnetic, magnetoelectric properties of the Ba_{0.9}Ca_{0.1}Ti_{0.9}Zr_{0.1}O₃/CoFe₂O₄ laminated composites. *J. Mater. Sci. Mater. Electron.* **28**, 11125–11131 (2017). <https://doi.org/10.1007/s10854-017-6899-1>

Publisher's Note Springer Nature remains neutral with regard to jurisdictional claims in published maps and institutional affiliations.